

# Chapter 2

## Turbulent Combustion: Concepts, Governing Equations and Modeling Strategies

Tarek Echekki and Epaminondas Mastorakos

**Abstract** The numerical modeling of turbulent combustion problems is based on the solution of a set of conservation equations for momentum and scalars, plus additional auxiliary equations. These equations have very well-defined foundations in their instantaneous and spatially-resolved forms and they represent a myriad of problems that are encountered in a very broad range of applications. However, their practical solution poses important problems. First, models of turbulent combustion problems form an important subset of models for turbulent flows. Second, the reacting nature of turbulent combustion flows imposes additional challenges of resolution of all relevant scales that govern turbulent combustion and closure for scalars. This chapter attempts to review the governing equations from the perspective of modern solution techniques, which take root in some of the classical strategies adopted to address turbulent combustion modeling. We also attempt to outline common themes and to provide an outlook where present efforts are heading.

### 2.1 Introduction

The subject of turbulent combustion spans a broad range of disciplines. The combination of the subject of turbulence on one hand and that of combustion already reveals the daunting task of predicting turbulent combustion flows. At the heart of the challenge is the presence of a broad range of length and time scales spanned by the various processes governing combustion and the degree of coupling between these processes across all scales.

Bilger et al. [4] have discussed the various paradigms that have evolved over the years to address the turbulent combustion problem. A running theme among these

---

Tarek Echekki  
North Carolina State University, Raleigh NC 27695-7910, USA, e-mail: [techekki@ncsu.edu](mailto:techekki@ncsu.edu)

Epaminondas Mastorakos  
Cambridge University, Cambridge, CB2 1PZ, UK, e-mail: [em257@eng.cam.ac.uk](mailto:em257@eng.cam.ac.uk)

paradigms is the separation of scales to overcome the coupled multiscale complexity of turbulent combustion flows. In many respects, these strategies have been successful for a large class of problems and enabled the use of computational fluid dynamics (CFD) for the prediction and design of combustion in practical devices. The review by Bilger et al. [4] also identified recent trends in turbulent combustion modeling. These trends are motivated and enabled by the need to represent important finite-rate chemistry effects and non-equilibrium chemistry effects in combustion. Requirements for combustion technologies only 20 years ago are not the same as the requirements we dictate now. A variety of alternative fuels are explored in addition to high grade fossil fuels. Pollution mitigation also enforces additional requirements on the choice of the fuel, its equivalence ratio and mixture control (e.g. homogeneity of the charge).

Additional qualitative changes in the scope of turbulent combustion models can be gaged from two seminal contributions in the field of turbulent combustion. They correspond to two contributed volumes entitled ‘Turbulent Reacting Flows’, which were edited by Libby and Williams in 1980 and 1994 [27, 28]. A comparison of the topics covered in the two books and the present volume illustrates important expansions in the scope of the field of turbulent combustion. The key areas of expansion are outlined here:

- The role of chemistry in turbulent combustion simulations has seen a tremendous growth since the Libby and Williams [27, 28] volumes. Already in the 1980’s software packages, such as Sandia’s Chemkin [20] chemistry and transport libraries and associated zero-dimensional and one-dimensional applications, have enabled important advances in the prediction of the role of finite-rate chemistry effects in combustion [9]. Because of the disparity of chemical scales, stiff-integration software were becoming available for the integration of chemistry, such as the DASSL [41] and VODE [5] software packages. These packages played an essential role in the implementation of chemistry in combustion problems. Beyond the traditional strategies of quasi-steady state assumptions (QSSA) for species and partial equilibrium (PE) for reactions and sensitivity analysis, novel numerical tools have contributed to efficient strategies for the acceleration of chemistry in numerical codes. Examples of such strategies include mechanism automation strategies based on QSSA and PE [6], systematic eigenvalue based approaches, including the computational singular perturbation (CSP) [23] approach and the intrinsic low-dimensional manifold (ILDM) [47] approach, and direct relation graph [24]. Chapter 9 provides ample discussion on chemistry reduction and integration.
- Large-eddy simulation (LES) has emerged as an alternative mathematical framework for the solution of transport equations for momentum and scalars. The traditional strategy, which is more common, is based on Reynolds-averaged Navier-Stokes (RANS) and associated equations for scalar transport, is not always sufficient for complex flows. LES has seen tremendous growth in the 1980’s for turbulent non-reacting canonical flows; but, it is increasingly becoming a viable modeling framework for practical combustion flows. LES potentially enables accurate solutions of combustion flows incorporating unsteady flow effects.

Successful LES simulations with advanced combustion models are increasingly being used to model practical combustion devices [49].

- A broader range of combustion modes (e.g. premixed, non-premixed, stratified) and combustion regimes (e.g. thin or relatively thick reaction zones) are being explored in current and novel combustion technologies. The strict classification of combustion modes as either premixed or non-premixed, while powerful for the development of physical models of turbulent combustion, may not be separately adequate to represent partially-premixed combustion modes. Combustion in stratified mixture plays key role in a number of practical combustion applications, including diesel, gas turbine and homogeneous charge compression ignition (HCCI) combustion. In his textbook, Peters [40] dedicates an entire chapter to partially-premixed combustion with the recognition of the role of this combustion mode in a broad range of combustion problems, and novel modeling strategies have been developed for this combustion regime.
- Moreover, earlier important advances in turbulent combustion concerned primarily phenomena in which the separation of scales can be justified, such as in the cases of fast chemistry and in the flamelet regime. For example, both the eddy-dissipation model (EDM) [31] and the flamelet model [39] demonstrated a broad range of applicability in predicting combustion in practical combustion devices. However, combustion in other regimes where both chemistry and mixing are competitive during ignition (e.g. HCCI combustion) and flame-based combustion (e.g. distributed reaction, corrugated flames), are more challenging.
- Both books by Libby and Williams [27, 28] adopt the traditional view that turbulent combustion modeling primarily is a physical modeling challenge. However, the increasing availability of computational resources has enabled further and accelerated development of direct numerical simulation (DNS) techniques for combustion. In a recent paper, Valorani and Paolucci [53] make the observation ‘No longer than 10 years ago, a direct numerical simulation (DNS) [11] of a turbulent flame with a four-step kinetics mechanism on a 10 mm box constituted the state-of-the-art in combustion simulation. Nowadays, the targets are DNSs of turbulent combustion of surrogate fuels, in half-a-meter domains.’ As stated in Chapter 1 and elsewhere in this book, DNS may not be applicable to practical combustion devices for some time to come. However, other DNS-like techniques have been used to model laboratory-scale burners, such as recent simulations based on adaptive mesh refinement (AMR) [1, 2].

Our current understanding of the fundamental laws governing reacting flows enables us to formulate detailed physical models, with minimum empiricism, for a large number of the processes underlying turbulent combustion. For example, atomistic simulations may be used to construct databases for rate constants and thermochemical and molecular transport properties of reacting species. But, atomistic approaches alone may not extend to the scales relevant to practical combustion problems; yet, with the help of constitutive relations derived for molecular processes, continuum-based formulations for reacting flows are a good starting point.

Even within the continuum limit, various strategies may be adopted. These strategies may reflect the formulation of the mathematical models for the governing equa-

tions as well as their numerical solution in addition to inherent simplification of these equations due to the flow regime (e.g. low Mach number formulations). They also reflect the scope of the modeler whether she/he is interested in statistical results or fully-resolved (spatially and temporally) results. The latter scope belongs to the realm of direct numerical simulations (DNS) where the governing equations are solved without filtering or averaging of the solution vector and with a full account of the required spatial and temporal resolution within the continuum limit. However, recourse to unsteady information is progressively seen also as one of the reasons for moving towards LES as in, for example, the effort to capture ignition or extinction phenomena [52]. The governing equations for DNS will be the starting point for discussing the different strategies adopted to address the mathematical models in turbulent combustion and their numerical solutions. Our emphasis is on two mathematical frameworks for representing the solution vector based on RANS and LES. Following effort in the turbulence community, other mathematical frameworks may be feasible as well, but RANS and LES are the most common approaches in modern turbulent combustion modeling and will form the focus of this book.

## 2.2 Governing Equations

### 2.2.1 Conservation Equations

The governing equations for turbulent combustion flows may be expressed in different forms; however, they normally are represented as transport equations for overall continuity, momentum and additional scalars that can be used to spatially- and temporally- resolve the thermodynamic state of the mixture. These equations are augmented by initial and boundary conditions, as well as constitutive relations for atomistic processes (e.g. reaction, molecular diffusion, equations of state). Therefore, in addition to density, transport equations for the evolving momentum and composition (e.g. mass or mole fractions, species densities or concentrations) and a scalar measure of energy (e.g. internal energy, temperature, or enthalpy). For illustration purposes, we present the compressible form of the instantaneous governing equations in non-conservative form for the mass density, momentum, species mass fractions and internal energy. A more detailed discussion on the various forms and their equivalence, especially for the energy equation can be found in the textbooks by Williams [57] or Poinso and Veynante [44].

- Continuity

$$\frac{\partial \rho}{\partial t} + \nabla \cdot \rho \mathbf{u} = 0, \quad (2.1)$$

- Momentum

$$\rho \frac{D\mathbf{u}}{Dt} = \rho \frac{\partial \mathbf{u}}{\partial t} + \rho \mathbf{u} \cdot \nabla \mathbf{u} = -\nabla p + \nabla \cdot \boldsymbol{\tau} + \rho \sum_{k=1}^N Y_k \mathbf{f}_k, \quad (2.2)$$

- Species continuity ( $k = 1, \dots, N$ )

$$\rho \frac{DY_k}{Dt} = \rho \frac{\partial Y_k}{\partial t} + \rho \mathbf{u} \cdot \nabla Y_k = \nabla \cdot (-\rho \mathbf{V}_k Y_k) + \omega_k, \quad (2.3)$$

- Energy

$$\rho \frac{De}{Dt} = \rho \frac{\partial e}{\partial t} + \rho \mathbf{u} \cdot \nabla e = -\nabla \cdot \mathbf{q} - p \nabla \cdot \mathbf{u} + \boldsymbol{\tau} : \nabla \mathbf{u} + \rho \sum_{k=1}^N Y_k \mathbf{f}_k \cdot \mathbf{V}_k. \quad (2.4)$$

In the above equations,  $\rho$  is the mass density;  $\mathbf{u}$  is the velocity vector;  $p$  is the pressure;  $\mathbf{f}_k$  is the body force associated with the  $k$ th species per unit mass;  $\boldsymbol{\tau}$  is the viscous stress tensor;  $\mathbf{V}_k$  is the diffusive velocity of the  $k$ th species, where the velocity of the  $k$ th species may be expressed as the sum of the mass-weighted velocity and the diffusive velocity,  $\mathbf{u} + \mathbf{V}_k$ ;  $\omega_k$  is the  $k$ th species production rate;  $e$  is the mixture internal energy, which may be expressed as  $e = \sum_{k=1}^N h_k Y_k - p/\rho$ ;  $\mathbf{q}$  is the heat flux, which represents heat conduction, radiation, and transport through species gradients and the Soret effect. The solution vector,  $\Xi$  represented by the above governing equations (2.1)–(2.4) is  $\Xi = (\rho, \rho \mathbf{u}, \rho \mathbf{Y}, \rho e)$  in its conservative form or  $\Xi = (\rho, \mathbf{u}, \mathbf{Y}, e)$  in its non-conservative form. The governing equations may be expressed in a more compact form as follows:

$$\frac{D\Xi}{Dt} = \mathbf{F}(\Xi) \quad (2.5)$$

where  $\mathbf{F}(\Xi)$  represents the right-hand side of the governing equations and features terms with spatial derivatives (e.g. diffusive fluxes for mass and heat) and source terms (e.g. reaction source terms). The material derivative  $D\Xi/Dt$  includes both the unsteady term and the advective term in the Eulerian representation such that:  $D\Xi/Dt \equiv \partial \Xi / \partial t + \mathbf{u} \cdot \nabla \Xi$ . As can be seen, a number of terms in the governing equations are not explicitly expressed in terms of the solution vector and must rely on constitutive relations, equations of state or any additional auxiliary relations. These terms include expressions for the viscous stress, the species diffusive velocities, the body forces, the species reaction rate and the heat flux. The bulk of these terms have their origin in the molecular scales, and therefore, the role of constitutive relations is to represent them in continuum models. In fact, the use of constitutive equations is the first level of multiscale treatment for the modeling of turbulent combustion flows. Alternative, but significantly more costly approaches, involve their determination using atomistic models coupled ‘on the fly’ with continuum models. However, cases where such approaches are needed are very limited.

## 2.2.2 Constitutive Relations, State Equations and Auxiliary Relations

### 2.2.2.1 Constitutive Relations, Transport Properties and State Equations

The constitutive relations for the conservation equations outlined above represent primarily relations between transport terms for momentum, energy and species and the solution vector as well as relations that describe the rate of chemistry source terms in the species equations. They are designed to represent atomistic scale effects of transport and reaction. Below we outline the principal terms that are represented by constitutive relations.

- The pressure and viscous stress tensor: In gas-phase flows applicable to combustion problems, the Newtonian fluid assumption is reasonably valid, and the viscous stress tensor may be represented through the following relation:

$$\boldsymbol{\tau} = \mu \left[ (\nabla \mathbf{u}) + (\nabla \mathbf{u})^T \right] + \left( \frac{2}{3} \mu - \kappa \right) (\nabla \cdot \mathbf{u}) \mathbf{I} \quad (2.6)$$

In this expression,  $\mu$  is the dynamic viscosity;  $\kappa$  is the bulk viscosity; and  $\mathbf{I}$  is the identity matrix. The principle of corresponding states provides generalized curves for the viscosity of gases, liquids and supercritical fluids for a broad range of temperature and pressure conditions. The principle states that a reduced viscosity, based on the ratio of the dynamic viscosity to that at critical conditions, may be uniquely defined in terms of a reduced temperature and pressure, both reduced values result from the normalization of temperature and pressure with their corresponding critical values.

- The diffusive mass flux,  $\rho Y_k \mathbf{V}_k$ : The diffusive mass flux represents the transport of species in addition to their transport with the bulk flow,  $\mathbf{u}$ . Diffusive mass transport may be associated with gradients in mass or species concentration, the so-called Fickian diffusion, temperature gradients, or the so-called Dufour effect, and pressure gradient. A hierarchy of models for the diffusive mass flux may be adopted. The first is based on adopting a Fick's law model using mixture-averaged transport coefficients:

$$X_k \mathbf{V}_k = -D_k^m \nabla X_k \quad (2.7)$$

where  $D_k^m$  is the mixture-averaged mass diffusion coefficient for species  $k$ . The mixture-averaged mass diffusion coefficient is derived, in general, using mixture weighting rules and multi-component diffusion coefficients. A simple form of the mixture-averaged diffusivity is based on the assumption of constant diffusion coefficients' ratios (e.g. fixed Lewis numbers or Schmidt numbers), such that the mixture-averaged mass diffusion coefficient is expressed as follows [50]:

$$D_k^m = \frac{\lambda}{\rho c_p Le_k} \quad (2.8)$$

where  $c_p$  is the mixture specific heat;  $\lambda$  is the mixture thermal conductivity; and  $Le_k$  is the  $k$ th species Lewis number.

The second approach is based on a multi-component formulation [8]:

$$\mathbf{V}_k = \frac{1}{X_k W} \sum_{j=1, j \neq k}^N W_j D_{kj} \mathbf{d}_j - \frac{D_{T,k}}{\rho Y_k} \frac{1}{T} \nabla T \quad (2.9)$$

In this expression,  $D_{kj}$  and  $D_{T,k}$  are the binary mass diffusivity between species  $k$  and  $j$  and the thermal diffusion coefficient, respectively;  $\mathbf{d}_j$  is the concentration and pressure gradients for species  $j$ :

$$\mathbf{d}_j = \nabla X_j + (X_j - Y_j) \frac{\nabla P}{p} \quad (2.10)$$

Detailed formulations for  $D_{kj}$  and  $D_{T,k}$  may be found in various textbooks (see for example, Kee et al. [21]).

- The heat flux vector,  $\mathbf{q}$ : The heat flux vector  $\mathbf{q}$  features contributions from different modes of heat transfer, including heat conduction, heat diffusion by mass diffusion of the various species, thermal diffusion (Dufour effect), and radiative heat transfer. A general form of the heat flux featuring the contribution of these different heat transfer modes may be written as follows:

$$\mathbf{q} = -\lambda \nabla T + \rho \sum_{i=1}^N h_i Y_i \mathbf{V}_i + R_u T \sum_{i=1}^N \sum_{j=1}^N \left( \frac{X_j D_{T,i}}{W_i D_{ij}} \right) (\mathbf{V}_i - \mathbf{V}_j) + \mathbf{q}_{rad} \quad (2.11)$$

In this equation,  $\lambda$  is the mixture thermal conductivity and  $\mathbf{q}_{rad}$  is the radiative heat flux.

- The chemical reaction term,  $\omega_k$ : This term is derived from the law of mass action, which dictates that the rate of chemical reactions is proportional to the concentrations of the contributing species. The proportionality factor is primarily a function of temperature and is denoted as the reaction rate constant. Contributions to this term include statistical information about the rates of collisions, and the fraction of collisions resulting in reactions as well as steric factor, which take into consideration the shapes of molecules during collisions. The following equation represents the rate of production of species  $k$  due to its involvement in  $R$  reversible reactions:

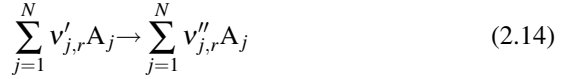
$$\omega_k = W_k \sum_{r=1}^R \left\{ (v''_{k,r} - v'_{k,r}) \left[ k_{f,r} \prod_{j=1}^N \left( \frac{X_j P}{R_u T} \right)^{v'_{j,r}} - k_{b,r} \prod_{j=1}^N \left( \frac{X_j P}{R_u T} \right)^{v''_{j,r}} \right] \right\}, \quad (2.12)$$

where

$$k_{f,r}(T) = A_r T^{\alpha_r} \exp\left(\frac{-E_{a,r}}{R_u T}\right), k_{b,r} = \frac{k_{f,r}}{K_{C,r}} \quad (2.13)$$

In these expressions,  $W_k$  is the molecular weight for species  $k$ ;  $v'_{j,r}$  and  $v''_{j,r}$  are the  $r$ th reaction stoichiometric coefficients on the reactants and the products sides,

respectively;  $k_{f,r}$  and  $k_{b,r}$  are the forward and backward rate constants for the reversible reaction,  $r$ . The backward reaction rate constant is related to the forward rate constant through the concentration-based equilibrium constant,  $K_{C,r}$  for reaction  $r$ . In the Arrhenius form for the forward rate constant expression,  $A_r$  and  $\alpha_r$  are the pre-exponential coefficients, and  $E_{a,r}$  is the activation energy for the forward reaction,  $r$ . An elementary reaction,  $r$ , is prescribed as follows:



where  $A_j$  is the  $j$ th species chemical symbol.

The integration of the chemical source term in the species equation (as well as in the temperature or sensible enthalpy forms of the energy equation) poses important and limiting challenges in computational combustion, as discussed below.

The determination of transport properties for momentum, mass and energy remains an understated challenge. Various software packages for the evaluation of transport properties are available, including MIXRUN [56], TRANLIB [19], EGLIB [13] and DRFM [38]. A first challenge is to assemble reliable data for potential parameters that contribute to the evaluation of the collision integrals. Paul [38] find that special attention needs to be made in determining the transport properties for molecules with dipole moments (e.g. H atom,  $H_2$  molecule) and indeed numerical simulations with different levels of modeling transport can lead to different results.

### 2.2.2.2 Mixture Properties and State Equations

State equations enable to evaluate thermodynamic properties from known properties. A common relation involves the ideal gas law:

$$p = \rho R_u T \sum_{j=1}^N \left( \frac{Y_j}{W_j} \right) \quad (2.15)$$

The caloric equation of state may be used to relate a species enthalpy or internal energy to temperature as follows:

$$h_k(T) = h_{k,chem} + \int_{T^\circ}^T c_{p,k} dT \quad (2.16)$$

and

$$e_k(T) = h_{k,chem} + \int_{T^\circ}^T c_{v,k} dT \quad (2.17)$$

where  $h_k$  and  $e_k$  are the  $k$ th species total enthalpies and internal energies;  $T^\circ$  is a reference temperature for the sensible enthalpy. Here,  $h_{k,chem}$  corresponds to the chemical enthalpy of the  $k$ th species, and the second terms on the right hand-sides



of the two above equations corresponds to the sensible contributions;  $c_{v,k}$  and  $c_{p,k}$  are the specific heats for species  $k$  at constant volume and pressure, respectively.

### 2.2.2.3 Other Transport Equations

Along with, or instead of, the scalar transport equations, transport equations for additional scalars may be used. These include conserved scalars (e.g. mixture fraction, total enthalpy), normalized reaction progress variables and flame surface variables (e.g. flame surface density).

Conserved scalars may be found in different aspects of combustion analysis from theory to experiment. They offer the convenience that their transport equations are devoid of source terms. Therefore, their integration is not subject to the steep time constraints of integrating chemistry. The Shvab-Zeldovich [57] formulation offers an early example of the use of conserved scalars in the limit of fast chemistry in terms of the so-called ‘coupling functions’. The same concept based on this formulation resulted in one of the classic analytical solutions in combustion based on the Burke-Schumann jet flame model [57]. However, the concepts of elemental mass fractions and mixture fractions have offered significantly more insight into processes in turbulent combustion, especially in non-premixed combustion. From a mixture composition, it is possible to construct an elemental mass fraction,  $Z_l$ , for element  $l$ , which may be prescribed as:

$$Z_l = \sum_{j=1}^N \mu_{j,l} Y_j \quad (2.18)$$

where  $\mu_{j,l}$  is the mass fraction of element  $l$  in species  $j$ . The elemental mass fraction is unaltered by reaction; and therefore, there is no source term associated with its transport equation:

$$\rho \frac{DZ_l}{Dt} = \rho \frac{\partial Z_l}{\partial t} + \rho \mathbf{u} \cdot \nabla Z_l = \nabla \cdot (-\rho \mathbf{V}_l Z_l). \quad (2.19)$$

Here, the diffusive velocity associated with the elemental mass fraction is expressed as follows:

$$\sum_{j=1}^N \mathbf{V}_j \mu_{j,l} Y_j = \mathbf{V}_l Z_l \quad (2.20)$$

The mixture fraction represents a normalized form of the elemental mass fraction, and it is a parameter of great value for non-premixed chemical systems. It measures the fraction by mass in the mixture of the elements, which originates in the fuel. When derived from elemental mass fractions, it may be expressed in normalized form as:

$$F_l = \frac{Z_l - Z_{l,o}}{Z_{l,f} - Z_{l,o}} \quad (2.21)$$

where the subscripts  $o$  and  $f$  refer to the oxidizer and the fuel mixture conditions, respectively. In a mixing system of fuel and oxidizer streams, values of the mixture fractions based on different elements may be different because of differential diffusion effects. Element-averaged mixture fractions, such as the Bilger mixture fraction [3], may be adopted:

$$F_{\text{Bilger}} = \frac{2(Z_C - Z_{C,o})/W_C + (Z_H - Z_{H,o})/(2W_H) - (Z_O - Z_{O,o})/W_O}{2(Z_{C,f} - Z_{C,o})/W_C + (Z_{H,f} - Z_{H,o})/(2W_H) - (Z_{O,f} - Z_{O,o})/W_O} \quad (2.22)$$

where the subscripts C, H and O correspond to the elements C, H and O, respectively, and the symbol  $W$  refers to their corresponding molar masses. The coefficients in front of the different elemental contributions serve the important role of maintaining the stoichiometric Bilger mixture fraction value identical to the elemental mixture fractions. As stated earlier, the mixture fraction is an important parameter for the modeling of non-premixed systems [3, 40, 57].

## 2.3 Conventional Mathematical and Computational Frameworks for Simulating Turbulent Combustion Flows

Within the continuum limit, there are different mathematical and computational frameworks to model turbulent combustion flows. These frameworks address the way the governing equations are modified and the way the solutions are implemented computationally (e.g. discretization). Strategies to overcome the limitations of resolving all the time and length scales even within the continuum limit motivates two principal classes of modeling frameworks associated with model-adaptivity or mesh-adaptivity or both. Model adaptivity refers to a class of models in which the governing equations, and accordingly the solution vector  $\Xi$ , are modified to a reduced order, a reduced dimension, or a statistical form, which effectively decouples or eliminates ranges of scales from the solution vector. Mesh adaptivity refers to a class of models in which the solution vector,  $\Xi$ , is resolved by adapting the grid hierarchy or the resolution hierarchy where it is needed to meet prescribed error criteria.

As indicated above, model adaptivity is concerned with modifying the governing equation and the solution vector. For combustion flows, three principal strategies have been implemented for model adaptivity; while, potentially other approaches may be considered. They correspond to DNS, RANS and LES.

### 2.3.1 Direct Numerical Simulation (DNS)

DNS corresponds to the solution of the 3D unsteady governing equations (Eqs. 2.1–2.4) with the necessary resolution required to accurately integrate the solution in

time and predict the details of velocity and scalar fields. Therefore, DNS offers the best resolved framework for the study of turbulent combustion flows. A typical 3D unsteady DNS in combustion must span the ranges of time and length scales discussed above (approximately 4-5 decades in length scales within the continuum regime in a given direction), which entail resolution requirements of the order of trillions of grid points or higher and tens of millions of time steps. Yet, the state-of-the-art DNS of combustion have been limited to computational domains that are approximately one order of magnitude smaller in linear scale (or three orders of magnitude in volume) than laboratory flames or practical combustion devices. However, achieving these length scales is fast approaching with petascale capabilities and beyond. Nonetheless, DNS remains a powerful tool to understand important turbulence-chemistry interaction processes and formulate closure models in turbulent combustion [43, 54, 55]. Computational requirements for DNS may vary depending on the level of description of the chemistry, molecular transport and radiation as well as the representation of the governing equations (e.g. low-Mach number formulation vs. compressible formulations). Examples of computational requirements may be found in a recent paper by Chen et al. [7].

A principal challenge for DNS remains the temporal integration of the conservation equations, especially those pertaining to the integration of the reactive scalars. A temporal resolution from the fastest reactions (of the order of  $10^{-9}$  s for hydrocarbon chemistry) to integral scales of the flow results in hundreds of thousands to million time steps with explicit integration schemes; accordingly, DNS simulations remain largely CPU-limited. Lu and Law [29] present an analysis of the cost of integrating chemistry within DNS. Their analysis shows that:

- The size of a chemical mechanism (i.e. the number of reactions) increases approximately linearly with the number of chemical species considered; the scaling factor is approximated as 5 between the chemical mechanism size and the number of species involved. This scaling is presented for hydrocarbon fuels. However, it is clear that as DNS applications are extended from hydrogen and simple hydrocarbon fuels to more common fuels (e.g. gasoline, diesel, kerosene), additional cost is associated with both the transport of more scalar equations as well as in the evaluation and the integration of non-linear reaction rate terms. The task is daunting given that more than one order of magnitude separates the size of simple and more complex fuel chemistries.
- The computational cost of DNS at each grid,  $C_{DNS}$ , also scales approximately linearly with the number of species,  $N$ , involved:  $C_{DNS} \propto N$ . The proportionality factor subsumes contributions associated with the spatial resolution and the cost of advancing the scalar transport equations, including the evaluation of transport properties and chemical reaction rates.

Therefore, aggressive strategies for chemistry reduction are warranted and may need to go beyond the development of skeletal mechanisms. Additional strategies for chemistry calculation acceleration are needed equally to overcome the stiff chemistry. These strategies have been pursued and significant progress has been achieved in recent years. An additional challenge is to account for the transport of

tens to hundreds of species in mechanisms that range in size from tens to thousands of reactions. The subject of chemistry reduction and acceleration has received increasing interest in recent years (see for example the recent reviews by Lu and Law [29] and Pope and Ren [48]). Chapter 9 details further strategies for chemistry reduction and acceleration.

Another equally important effort is to address spatial resolution requirements. Spatial resolution must resolve the thinnest layers of reaction zone structures; these layers represent the balance of reaction and diffusion and at their thinnest may be of the order of  $10 \mu\text{m}$  or smaller. It is difficult to justify not to resolve these layers if they serve a role in the combustion process; and often strategies to address the resolution of these layers may be implemented through adapting the spatial resolutions where these layers are present and coarsening the resolution when such fine resolutions are not needed. Adaptive resolution strategies offer the most promising strategies for addressing spatial resolution and often result in almost an order of magnitude gain in the size of problems to be solved in comparison with DNS. Typical examples of mesh adaptivity include adaptive mesh refinement (AMR), which is discussed in Chapter 13 and wavelet-based adaptive multiresolution strategies, which are discussed in Chapter 14.

### 2.3.2 Reynolds-Averaged Navier-Stokes (RANS)

The Reynolds-averaged Navier-Stokes (RANS) formulation is based on time or ensemble averaging of the instantaneous transport equations for mass, momentum and reactive scalars. Within the context of scale separation, the RANS approach indiscriminately impacts all scales. Consequently, all unsteady turbulent motion and its coupling with combustion processes are unresolved over the entire range of length and time scales of the problem, and closure models are needed to represent the unresolved physics. An additional complexity introduced by averaging is that non-linear terms in the governing equations result in unclosed terms. The closure problem is particularly critical for the reaction source terms in the species and some forms of the energy equations. The treatment of these terms has been the scope of the moment-based methods. We illustrate the closure problem using the transport equation for the conservation equations above (Eqs. 2.1–2.4). Before listing the conservation equations, we briefly address the advantages of density-weighted averaging or the so-called Favre-averaging [14, 18]. With Favre-averaging, all momentum and scalars, at the exception of the density, the pressure and diffusive fluxes, are decomposed using a Favre-averaged means and fluctuations:

$$\Xi = \tilde{\Xi} + \Xi' \quad (2.23)$$

The Favre average,  $\tilde{\Xi}$  may be expressed in terms of the non-weighted average as:

$$\tilde{\Xi} \equiv \frac{\overline{\rho \Xi}}{\bar{\rho}} \quad (2.24)$$

The contribution  $\Xi'$  corresponds to the fluctuating components of the solution vector  $\Xi$  relative the Favre mean. The overbar denotes an unweighted ensemble average over a statistically-meaningful set of realizations; the symbol ' $\sim$ ' denotes a density-weighted ensemble average. Density-weighted averaging eliminates the need to explicitly represent the density-momentum and density-scalar correlations, which when kept in the governing equations generate additional closure terms. Based on the above conservation equations, the Favre-averaged continuity, momentum and scalar equations are expressed as follows:

- Continuity

$$\frac{\partial \bar{\rho}}{\partial t} + \nabla \cdot \bar{\rho} \tilde{\mathbf{u}} = 0, \quad (2.25)$$

- Momentum

$$\bar{\rho} \frac{\partial \tilde{\mathbf{u}}}{\partial t} + \bar{\rho} \tilde{\mathbf{u}} \cdot \nabla \tilde{\mathbf{u}} = -\nabla \bar{p} + \nabla \cdot \bar{\boldsymbol{\tau}} + \bar{\rho} \sum_{k=1}^N \widetilde{Y_k \mathbf{f}_k} - \nabla \cdot (\bar{\rho} \widetilde{\mathbf{u}' \mathbf{u}'}), \quad (2.26)$$

- Species continuity ( $k = 1, \dots, N$ )

$$\bar{\rho} \frac{\partial \tilde{Y}_k}{\partial t} + \bar{\rho} \tilde{\mathbf{u}} \cdot \nabla \tilde{Y}_k = \nabla \cdot (-\bar{\rho} \widetilde{\mathbf{V}_k Y_k}) + \bar{\omega}_k - \nabla \cdot (\bar{\rho} \widetilde{\mathbf{u}' Y'_k}), \quad (2.27)$$

- Energy

$$\bar{\rho} \frac{\partial \tilde{e}}{\partial t} + \bar{\rho} \tilde{\mathbf{u}} \cdot \nabla \tilde{e} = -\nabla \cdot \tilde{\mathbf{q}} - \overline{p \nabla \cdot \mathbf{u}} + \overline{\boldsymbol{\tau} : \nabla \mathbf{u}} + \bar{\rho} \sum_{k=1}^N \widetilde{Y_k \mathbf{f}_k \cdot \mathbf{V}_k} - \nabla \cdot (\bar{\rho} \widetilde{\mathbf{u}' e'}). \quad (2.28)$$

In the RANS formulation, the solution vector is expressed as  $\bar{\Xi} = (\bar{\rho}, \tilde{\mathbf{u}}, \tilde{\mathbf{Y}}, \tilde{e})$ . Both the source term and the advective term are non-linear contributions to the governing equations for the species, and invariably these terms will be unclosed since there is no explicit transport equation used to solve them. Additional new terms in the governing equation correspond to the Reynolds stresses and fluxes:  $\bar{\rho} \widetilde{\mathbf{u}' \mathbf{u}'}$ ,  $\bar{\rho} \widetilde{\mathbf{u}' Y'_k}$  and  $\bar{\rho} \widetilde{\mathbf{u}' e'}$  which are also unclosed and must be modeled. It is quite common to treat this term as a turbulent diffusion term with a gradient model. The molecular diffusion term is also unclosed; but, its description may depend largely on how it is modeled and how its effects are prescribed with the reaction source term. It is also common to assume that the turbulent diffusion term is much larger than the molecular diffusion term in the governing equations and that the molecular diffusion term is often dropped from the above governing equations. This is not strictly true because these two transport terms may act on different scales. Therefore, the effects of molecular diffusion may still have to be represented (typically through the chemistry closure). Nonetheless, the most critical closure arises from modeling the reaction source term,  $\bar{\omega}_k$ .

To motivate the strategies adopted for the closure for  $\bar{\omega}_k$ , the statistical representation of this term is expressed as follows:

$$\overline{\omega}_k = \int_{\Xi} \omega_k(\boldsymbol{\psi}) f(\boldsymbol{\psi}) d\boldsymbol{\psi}. \quad (2.29)$$

In this expression,  $f(\boldsymbol{\psi})$  is the joint scalar probability density function (PDF). The vector  $\boldsymbol{\psi}$  represents components of the thermodynamic state vector, which may include for example, pressure, temperature and composition. Therefore, the vector,  $\boldsymbol{\psi}$ , may be a subset of the solution vector,  $\Xi$ , which also includes the momentum components. The joint PDF contains the complete statistical information about all scalars. Therefore, the averaged scalar field, its moments and any related functions of the field may be constructed using this joint scalar PDF:

$$\overline{\Xi} = \int_{\boldsymbol{\psi}} \Xi(\boldsymbol{\psi}) f(\boldsymbol{\psi}) d\boldsymbol{\psi}, \quad (2.30)$$

and

$$\overline{\Omega(\Xi)} = \int_{\boldsymbol{\psi}} \Omega(\boldsymbol{\psi}) f(\boldsymbol{\psi}) d\boldsymbol{\psi}. \quad (2.31)$$

A density-weighted PDF may be defined as well, which may be written as follows:

$$\tilde{f}(\boldsymbol{\psi}) = \frac{\rho(\boldsymbol{\psi})}{\bar{\rho}} f(\boldsymbol{\psi}) \quad (2.32)$$

These expressions offer an important window into closure strategies in turbulent combustion within the context of RANS. An accurate description of averaged scalars, their moments and functions of these moments must involve an accurate account of the state-vector solution (i.e. the instantaneous correlation,  $\Xi(\boldsymbol{\psi})$  inside the integral) as well as an accurate account of the statistical distribution,  $f(\boldsymbol{\psi})$ . Often, the modeling of the two contributions is coupled, and the choice of the combustion mode or regime may enable strategies for the modeling of the state-vector solutions as well as the joint scalar PDF.

### 2.3.3 Large-Eddy Simulation (LES)

The third approach is based on spatially filtering the instantaneous equations to capture the contribution of large scales, resulting in transport equations for spatially filtered mass, momentum and scalars, while the effects of smaller scales are modeled. This approach is known as large-eddy simulation [42]. LES relies on scale separation between (kinetic) energy containing eddies and small scales responsible for its dissipation (the so-called subgrid scale, or SGS). The approach is rooted in the traditional view of turbulent flows where the bulk of turbulent kinetic energy originates at the large scales; however, this choice has limited justification in combustion flows: important physics may reside and originate at small scales.

From a modeling standpoint, LES provides a number of important advantages towards the prediction of turbulent combustion flows over RANS. First, LES captures large scale information in both the momentum and scalar fields. Therefore, it is able

to capture the role of large flow structures on mixing and, therefore, on combustion. These flow structures are inherently unsteady, and capturing their interactions with combustion chemistry is very crucial in a broad range of practical applications. For example, tumble and swirl in internal combustion engines serve to enhance the volumetric rate of heat release and contribute to cycle-to-cycle variations. Moreover, the lift-off and blow-out of lifted flames in practical burners is dependent on the unsteady flow dynamics around the flame leading edge and the inherent instabilities in the presence of shear. Another example is associated with the prediction of thermo-acoustic and other flow-associated instabilities in gas turbine combustors.

Second, because LES is designed to capture the role of a band of scales, it can naturally be implemented within the context of multiscale frameworks. In these frameworks, simulations of the subgrid scale physics is implemented along with LES to capture the contributions from all relevant scales. Hybrid approaches of LES with low-dimensional stochastic models, such as the LEMLES and the ODTLES frameworks discussed in Chapters 10 and 11 illustrate the implementation of LES for combustion within the context of multiscale approaches. However, as outlined in this book and briefly discussed above, LES is a promising strategy within the context of moment-based approaches, such as non-premixed and premixed flames (Chapters 3 and 4), the conditional moment closure (CMC) model (Chapter 5), the transported PDF (Chapter 6), and the multiple mapping conditioning (MMC) approach (Chapter 7).

Third, since closure in LES targets primarily subgrid scale physics, a higher degree of universality in statistics may be achieved when the contribution from geometry-dependent large scales are eliminated from consideration.

We consider a filtering operation applied to the conservation equations. The filtering operation corresponds to the implementation of a low-pass filter, which is expressed as follows for a solution vector component,  $\Xi$ :

$$\overline{\Xi}(\mathbf{x}, t) = \int_{\Delta} G(\mathbf{x}, \mathbf{x}') \Xi(\psi; \mathbf{x}', t) d\mathbf{x}' \quad (2.33)$$

In this expression,  $G$  is a filtering function over 3D space with a characteristic scale,  $\Delta$ , the filter size. Similarly to the RANS formulation for variable-density flows, the filtered solution vector, at the exception of the filtered density, is based on density-weighted filtering, such that:

$$\tilde{\Xi}(\psi; \mathbf{x}, t) \equiv \frac{\overline{\rho \Xi}}{\overline{\rho}} \quad (2.34)$$

where

$$\overline{\rho \Xi} = \int_{\Delta} G(\mathbf{x}, \mathbf{x}') \rho(\psi; \mathbf{x}', t) \Xi(\psi; \mathbf{x}', t) d\mathbf{x}' \quad (2.35)$$

The Favre-filtered momentum and scalar equations are expressed as follows:

- Continuity

$$\frac{\partial \bar{\rho}}{\partial t} + \nabla \cdot \bar{\rho} \tilde{\mathbf{u}} = 0, \quad (2.36)$$

- Momentum

$$\bar{\rho} \frac{\partial \tilde{\mathbf{u}}}{\partial t} + \bar{\rho} \tilde{\mathbf{u}} \cdot \nabla \tilde{\mathbf{u}} = -\nabla \bar{p} + \nabla \cdot \bar{\boldsymbol{\tau}} + \bar{\rho} \sum_{k=1}^N + \bar{\rho} \sum_{k=1}^N \widetilde{Y_k \mathbf{f}_k} + \nabla \cdot [\bar{\rho} (\tilde{\mathbf{u}} \tilde{\mathbf{u}} - \mathbf{u} \mathbf{u})], \quad (2.37)$$

- Species continuity ( $k = 1, \dots, N$ )

$$\bar{\rho} \frac{\partial \tilde{Y}_k}{\partial t} + \bar{\rho} \tilde{\mathbf{u}} \cdot \nabla \tilde{Y}_k = \nabla \cdot (-\bar{\rho} \widetilde{\mathbf{V}_k Y_k} + \bar{\omega}_k + \nabla \cdot [\bar{\rho} (\tilde{\mathbf{u}} \tilde{Y}_k - \mathbf{u} Y_k)]), \quad (2.38)$$

- Energy

$$\bar{\rho} \frac{\partial \tilde{e}}{\partial t} + \bar{\rho} \tilde{\mathbf{u}} \cdot \nabla \tilde{e} = -\nabla \cdot \tilde{\mathbf{q}} - \overline{p \nabla \cdot \mathbf{u}} + \overline{\boldsymbol{\tau} : \nabla \mathbf{u}} + \bar{\rho} \sum_{k=1}^N \widetilde{Y_k \mathbf{f}_k} \cdot \mathbf{V}_k + \nabla \cdot [\bar{\rho} (\tilde{\mathbf{u}} \tilde{e} - \mathbf{u} e)]. \quad (2.39)$$

We have kept the same symbols for operations as above, although they correspond to spatial filtering operations instead of ensemble or time-averaging as in RANS. Here the overbar corresponds to a process of unweighted spatial filtering and the ‘ $\tilde{\cdot}$ ’ corresponds to a density-weighted spatial filtering. Again, considering the revised solution vector,  $\tilde{\Xi} = (\bar{\rho}, \tilde{\mathbf{u}}, \tilde{\mathbf{Y}}, \tilde{e})$ , additional terms are present in the governing equation, which correspond to subgrid scale stresses  $\bar{\rho} (\tilde{\mathbf{u}} \tilde{\mathbf{u}} - \mathbf{u} \mathbf{u})$  and scalar fluxes,  $\bar{\rho} (\tilde{\mathbf{u}} \tilde{Y}_k - \mathbf{u} Y_k)$  and  $\bar{\rho} (\tilde{\mathbf{u}} \tilde{e} - \mathbf{u} e)$ . These terms also are unclosed and require modeling. The molecular diffusion term,  $\nabla \cdot (-\bar{\rho} \widetilde{\mathbf{V}_k Y_k})$ , may be insignificant in the governing equation relative to the scalar flux on the LES resolution, it acts at scales that are fundamentally different from those of the scalar fluxes; and therefore, its contribution may be closely tied to the reaction source term and its closure. The process of averaging or filtering of the governing equations invariably leaves the contributions of the unresolved physics unclosed, and similar challenges of closure are found.

Similarly to the RANS formulation, an important closure term corresponds to the reaction source terms,  $\bar{\omega}_k$ . Here, a similar concept to the PDF may be used based on the filtered-density function (fdf) [15]:

$$\bar{\omega}_k = \int_{\Psi} \omega_k(\psi) F(\psi) d\psi \quad (2.40)$$

and

$$\overline{\Omega(\Xi)} = \int_{\Psi} \Omega(\Xi(\psi)) F(\psi) d\psi \quad (2.41)$$

Here  $F(\Xi)$  is the filtered-density function.

At this point, it is important to contrast the concepts of PDF, which discussed within the context of RANS, and fdf, which is discussed within the context of LES. We introduce the concept of a fine-grained PDF [30], which represents the



time- and spatially-resolved joint PDF. This fine-grained PDF may be expressed as follows:

$$\zeta(\psi, \phi(\mathbf{x}, t)) = \delta(\psi - \phi(\mathbf{x}, t)) = \prod_{\alpha=1}^{N_\psi} \delta(\psi_\alpha - \phi_\alpha(\mathbf{x}, t)) \quad (2.42)$$

The fine-grained PDF,  $\zeta(\psi, \phi(\mathbf{x}, t))d\psi$  represents probability that at  $\mathbf{x}$  and  $t$ , that  $\psi_\alpha \leq \phi_\alpha \leq \psi_\alpha + d\psi_\alpha$  for all values of  $\alpha$ . Within the context of RANS, the joint scalar PDF may be expressed as follows:

$$f(\phi; \mathbf{x}, t) = \overline{\zeta(\psi, \phi(\mathbf{x}, t))} \quad (2.43)$$

The FDF is expressed in terms of the fine-grained PDF as follows:

$$F = \int_{-\infty}^{+\infty} \zeta(\psi, \phi(\mathbf{x}, t)) G(\mathbf{x}, \mathbf{x}') d\mathbf{x}' \quad (2.44)$$

Therefore, the PDF represents a distribution built over time or ensembles of realizations of the scalar values at one single position,  $\mathbf{x}$ . In contrast, the FDF represents an instantaneous subfilter distribution of the same scalars over a prescribed filter volume.

The closure of the reaction source term is a principal modeling challenge in combustion LES; and often, strategies implemented for RANS have been extended to LES as well, as discussed in various chapters in this book.

## 2.4 Addressing the Closure Problem

The scope of turbulent combustion modeling is related to the representation of reactive scalar statistics. The traditional strategy is based on the RANS averaging framework. However, LES is becoming a viable framework for turbulent combustion models. The challenges are fundamentally similar. Averaging or filtering results in the closure problem for key terms in the conservation equations, including primarily the chemical source terms. The bulk of chapters in this book (Chapters 3–14) attempt to address the different approaches to turbulent combustion closure.

In a recent review, Bilger et al. [4] discussed traditional paradigms that defined turbulent combustion modeling over the last 40 or so years. Principal strategies resulting from these paradigms are based on either a 1) separation of scales and/or 2) separation of model elements that address the model description of moments of reactive scalars in terms of scalar description in state-space and model for the distribution (PDF or FDF) function. Examples of models based on the separation of scales include the assumption of fast chemistry (e.g. the eddy dissipation model (EDM) [31], the eddy break-up model (EBU) [51]) and the laminar flamelet model [39] where the flames thicknesses are below the energetic turbulence scales.

We illustrate the second strategy by revisiting the Eqs. (2.29) and (2.40). The mean or filtered reactions is constructed through a weighted average of the instan-

taneous reaction rate  $\omega_k(\psi)$  and the distribution,  $f(\psi)$  or  $F(\psi)$ . For the instantaneous reaction rate term, a ‘reactor’ model is needed that is representative of the state-space conditions encountered. For example, a flamelet library or CMC solutions may represent such reactor models. For the distribution description different strategies may be adopted depending on whether a reduced description of the state-space variables is available. For example, in the standard laminar non-premixed flamelet model and in CMC, models for the mean mixture fraction and its variance may be used to construct presumed shape PDF functions for reactive scalars. In the Bray-Moss-Libby (BML) model, a simple PDF function is adopted in terms of the reaction progress variable for premixed flames, although knowledge of the PDF shape is not always guaranteed. The more general form for the determination of the joint PDF involves the solution for a transport equation for the PDF and the FDF. However, intermediate strategies may be adopted as well. These include 1) the construction of PDF/FDF’s using independent stochastic simulations, or 2) optimally build PDF’s, such as the ones based on the statistically-most likely distribution [45]. The mapping closure approach (MMC; see Chapter 7) illustrates a strategy where a PDF transport equation is adopted for the construction of a statistical distribution and the CMC approach is used for the state-space relations.

Given the scope of the Bilger et al. [4] paper as related to paradigms in turbulent combustion, other modeling approaches have not been discussed; they will be presented here and the remaining chapters in the book will address them in more detail.

## 2.5 Outline of Upcoming Chapters

In this chapter, we have attempted to provide a brief outline of the challenges associated with turbulent combustion modeling. These challenges may be addressed by improved physical models of turbulent combustion processes; great strides have been made in the last two decades since the later contribution of Libby and Williams [28] and the more recent combustion literature. Moreover, rapid advances in computational sciences (hardware and algorithms) have fueled important advances in high-fidelity simulations of turbulent combustion flows that provide direct solutions of unresolved physics.

This book attempts to highlight recent progress in the modeling and simulation of turbulent combustion flows. It is divided into four parts, which include 1) two introductory chapters (Chapters 1 and 2) and 2) that motivate the growth of the disciplines associated with turbulent combustion flows from a societal and technological perspectives, 2) progress and trends in turbulent combustion models, 3) progress and trends in a new class of models based on multiscale simulation strategies, and 4) cross-cutting science that may be needed to move the subject forward. In Part II, emphasis is placed on recent progress in advanced combustion models, including the flamelet approach for non-premixed systems (Chapter 3), approaches for premixed combustion(Chapter 4), CMC (Chapter 5), MMC (Chapter 7) and the

PDF approach (Chapter 6). In Part III, emphasis is placed on multiscale strategies that seek to directly or indirectly compute subgrid scale physics. This part is preceded by an introductory chapter highlighting the driving motivation behind multiscale strategies in turbulent combustion. Topics covered in this part include the role of chemistry reduction and acceleration (Chapter 9), the linear-eddy model (LEM) (Chapter 10), the one-dimensional turbulence (ODT) model (Chapter 11), flame-embedding (Chapter 12), adaptive-mesh refinement (AMR) (Chapter 13), wavelet-based methods (Chapter 14). Our coverage of existing models in Parts I and II is admittedly incomplete; but, it provides a flavor of current state-of-the-art and trends in turbulent combustion models. This state-of-the-art can be contrasted with the general strategies adopted during the last three decades to gauge recent progress. Part IV addresses cross-cutting science, which include the basic tools to advance the discipline of turbulent combustion modeling. Experiment has played, and will continue to play, a central role in the development of new and the refinement of old strategies. The role of experiment is discussed in Chapter 15. From the computational side, two principal drivers for improving turbulent combustion modeling and simulation are addressed. The first chapter (Chapter 16) deals with the subject of uncertainty quantification as an emerging requirement to improve the ability of turbulent combustion modeling and simulation tools to predict practical flows. The second chapter (Chapter 17) addresses the need to develop effective strategies to build optimized software tools to predict turbulent combustion flows. Chapter 18 presents the homogeneous multiscale method (HMM) as a mathematical multiscale framework for turbulent combustion. Finally, Chapter 19 reviews the lattice-Boltzmann method (LBM), which represents a viable alternative to the standard Navier-Stokes equations for a large class of flows.

## References

1. Bell, J.B., Day, M.S., Shepherd, I.G., Johnson, M.R., Cheng, R.K., Grcar, J.F., Beckner, V.E., Lijewski, M.J.: Numerical simulation of a laboratory-scale turbulent V-flame. *Proc. Nat. Acad. Sci.* **102**, 10006–10011 (2005)
2. Bell, J.B., Day, M.S., Grcar, J.F., Lijewski, M.J., Driscoll, J.F., Filatyev, S.A.: Numerical simulation of laboratory-scale turbulent slot flame. *Proc. Combust. Inst.* **31**, 1299–1307 (2009)
3. Bilger, R.W.: The structure of turbulent nonpremixed flames. *Proc. Combust. Inst.* **22**, 475–488 (1988)
4. Bilger, R.W., Pope, S.B., Bray, K.N.C., Driscoll, J.F.: Paradigms in turbulent combustion research, *Proc. Combust. Inst.* **30**, 21–42 (2005)
5. Brown, P.N., Byrne, G.D., Hindmarsh, A.C.: VODE: A variable coefficient ODE solver. *SIAM J. Sci. Stat. Comput.* **10**, 1038–1051 (1989)
6. Chen, J.-Y.: A General procedure for constructing reduced reaction mechanisms with given independent relations, *Combust. Sci. Technol.* **57**, 89–94 (1988)
7. Chen, J.H., Choudhary A., de Supinski, B., DeVries, M., Hawkes, E.R., Klasky, S., Liao, W.K., Ma, K.L., Mellor-Crummey, J., Podhorszki, N., Sankaran, R., Shende, S., and Yoo, C.S.: Terascale direct numerical simulations of turbulent combustion using S3D. *Comput. Sci. Discovery* **2**, 015001 (2009)
8. Dixon-Lewis, G.: A FORTRAN computer code for the evaluation of gas-phase multicomponent transport properties. *Proc. Royal Soc.* **A304**, 111–134 (1968)

9. Dixon-Lewis, G.: Structure of laminar flames Proc. Combust. Inst. **23**, 305–324 (1990)
10. Dubois, T., Jauberteau, F., Temam, R.: Dynamic multilevel methods and the numerical simulation of turbulence, Cambridge University Press (1999)
11. Echekki, T., Chen, J.H.: Unsteady strain rate and curvature effects in turbulent premixed methane-air flames. Combust. Flame **106**, 184–202 (1996)
12. Eggenspieler, G., Menon, S.: Combustion and emission modelling near lean blow-out in a gas turbine engine. Prog. Comput. Fluid Dyn. **5** 281–297 (2005)
13. Ern, A., Giovangigli, V.: EGLIB: A general purpose FORTRAN library for multicomponent transport property evaluations, Software Manual (1986)
14. Favre, A.: Equations des gas turbulents compressible. J. Mec. **4**, 361–390 (1965)
15. Gao, F., O'Brien, E.E.: A large-eddy simulation scheme for turbulent reacting flows. Phys. Fluids **5**, 1282–1284 (1993)
16. Germano, M., Piomelli, U., Moin, P., Cabot, W.H.: A dynamic subgrid-scale eddy viscosity model. Phys. Fluids A **3**, 1760–1765 (1991)
17. Hawkes, E.R., Sankaran, R., Sutherland, J.C. and Chen, J.H.: Structure of a spatially developing turbulent lean methane-air Bunsen flame. Proc. Combust. Inst. **31**, 1291–1298 (2007)
18. Jones, W.P.: Models for turbulent flows with variable density and combustion. In Prediction Methods for Turbulent Flows, Kollman, W. ed., pp. 379–421. Hemisphere (1980)
19. Kee, R.J., Dixon-Lewis, G., Warnatz, J., Coltrin, M.E., Miller, J.A.: A FORTRAN computer code package for the evaluation of gas-phase multicomponent transport properties, SAND86-8246, Sandia National Laboratories (1986)
20. Kee, R.J., Rupley, F.M., and Miller, J.A.: Chemkin-II: A FORTRAN Chemical Kinetics Package for the Analysis of Gas-Phase Chemical Kinetics. Sandia National Laboratories Report No. SAND 89–8009 (1989)
21. Kee, R.J., Coltrin, M.E., Giarborg, P.: Chemically Reacting Flow: Theory and Practice, Wiley-Interscience, New Jersey (2003)
22. Kim, S.H., Pitsch, H.: Mixing characteristics and structure of a turbulent jet diffusion flame stabilized on a bluff-body. Phys. Fluids **18**, 075103 (2006)
23. Lam, S.H., Goussis, D.A.: Understanding complex chemical kinetics with the computational singular perturbations. Proc. Combust. Inst. **22**, 931–941 (1988)
24. Law, C.K.: On the applicability of direct relation graph to the reduction of reaction mechanisms. Combust. Flame **146**, 472–483 (2006)
25. Law, C.K.: Combustion Physics, Cambridge University Press, New York (2006)
26. Law, C.K.: Combustion at a crossroads: Status and prospects. Proc. Combust. Inst. **31**, 1–29 (2006)
27. Libby, P.A., Williams, F.A.: Turbulent Reacting Flows, Springer-Verlag, Heidelberg (1980)
28. Libby, P.A., Williams, F.A.: Turbulent Reacting Flows, Academic Press, London (1994)
29. Lu, T.F., Law, C.K.: Toward accommodating realistic chemistry in large-scale computations. Prog. Energy Combust. Sci. **35**, 192–215 (2009)
30. Lundgren, T.S.: Distribution of functions in the statistical theory of turbulence. Phys. Fluids **10**, 969 (1967)
31. Magnussen, B.F., Hjertager, B.H.: On mathematical modeling of turbulent combustion with special emphasis on soot formation and combustion. Proc. Combust. Inst. **16**, 719–729 (1976)
32. Mizobuchi, Y., Sinjo, J., Ogawa, S., Takeno, T.: A numerical study of the formation of diffusion flame islands in a turbulent hydrogen jet lifted flame. Proc. Combust. Inst. **30**, 611–619 (2005)
33. Mizobuchi, Y., Tachibana, S., Shinjo, J., Ogawa, S., Takeno, T.: A numerical analysis of the structure of a turbulent hydrogen jet lifted flame. Proc. Combust. Inst. **29**, 2009–2015 (2002)
34. Moin, P., Squires, K., Cabot, W., Lee, S.: A dynamic subgrid-scale model for compressible turbulence and scalar transport. Phys. Fluids A **3**, 2746–2757 (1991)
35. Navarrao-Martinez, S., Kronenburg, A., Di Mare, F., Conditional moment closure for large-eddy simulations. Flow Turbul. Combust. **75**, 245–274 (2005)
36. McIlroy, A., McRae, G., Sick, V., Siebers, D.L., Westbrook, C.K., Smith, P.J., Taatjes, C., Trouve, A., Wagner, A.E., Rohlfling, E., Manley, D., Tully, F., Hilderbrandt, R., Green, W.,

- Marceau, D., O'Neal, J., Lyday, M., Cebulski, F., Garcia, T.R., Strong, D., Basic research needs for clean and efficient combustion of 21st century transportation fuels. Department of Energy Office of Science Report (2006)
37. Patel, N., Kirtas, M., Sankaran, V., Menon, S.: Simulation of spray combustion in a lean-direct injection combustor. *Proc. Combust. Inst.* **31**, 2327–2334 (2007)
  38. Paul, P.H.: DFRM: A new package for the evaluation of gas-phase transport properties, SAND98-8203, Sandia National Laboratories (1997)
  39. Peters, N.: Local quenching due to flame stretch and non-premixed turbulent combustion. *Combust. Sci. Technol.* **30**, 1–17 (1983)
  40. Peters, N.: *Turbulent Combustion*, Cambridge University Press, UK (2000)
  41. Petzold, L.R., A description of dassl: A differential/algebraic system solver, SAND82-8637, Sandia National Laboratories (1982)
  42. Pitsch, H., Large-eddy simulation of turbulent combustion. *Ann. Rev. Fluid Mech.* **38**, 453–482 (2006)
  43. Poinso, T., Candel, S., Trounev A.: Applications of direct numerical simulation to premixed turbulent combustion. *Prog. Energy Combust. Sci.* **21**, 531–576 (1995)
  44. Poinso, T., Veynante, D., *Theoretical and Numerical Combustion*, Second Ed., RT Edwards (2005)
  45. Pope, S.B.: The statistical theory of turbulent flames. *Philos. Trans., Roy. Soc. London Ser. A* **291**, 529–568 (1979)
  46. Pope, S.B.: Computations of turbulent combustion: Progress and challenges. *Proc. Combust. Inst.* **23**, 591–612 (1990)
  47. Pope, S.B., Maas, U.: Simplifying chemical kinetics: Intrinsic low-dimensional manifolds in composition space. *Combust. Flame* **88**, 239–264 (1992)
  48. Pope, S.B., Ren, Z.: Efficient implementation of chemistry in computational combustion. *Flow Turbul. Combust.* **82**, 437–453 (2009)
  49. Selle, L., Lartigue, G., Poinso, T., Koch, R., Schildmacher, K.: Compressible large eddy simulation of turbulent combustion in complex geometry on unstructured meshes. *Combust. Flame* **137**, 489–505 (2004)
  50. Smooke, M.D., Giovangigli, V.: *Reduced Kinetic Mechanisms and Asymptotic Approximations for Methane-Air Flames*. Lecture Notes in Physics, Springer-Verlag, Berlin **384** (1991)
  51. Spalding, D.B.: Mixing and chemical reaction in steady confined turbulent flames *Proc. Combust. Inst.* **13**, 649–657 (1971)
  52. Triantafyllidis, A., Mastorakos, E., Eggels, R.L.G.M.: Large eddy simulations of forced ignition of a non-premixed bluff-body methane flame with conditional moment closure. *Combust. Flame* **156**, 2328–2345 (2009)
  53. Valorani, M., Paolucci, S.: The G-scheme: A framework for multi-scale adaptive model reduction. *J. Comput. Phys.* **228**, 4665–4701 (2009)
  54. Vervisch, L., Poinso, T.: Direct numerical simulation of non-premixed turbulent flames. *Ann. Rev. Fluid Mech.* **30**, 655–691 (1998)
  55. Veynante, D., Vervisch, L.: Turbulent combustion modeling. *Prog. Energy Combust. Sci.* **28**, 193–266 (2002)
  56. Warnatz, J.: Calculation of structure of laminar flat flames. 1. Flame velocity of freely propagating ozone decomposition flames. *Ber. Bunsenges. Phys. Chem. Phys.* **82**, 193–200 (1978)
  57. Williams, F.A., *Combustion Theory: The Fundamental Theory of Chemically Reacting Flow Systems*, Second Ed., Benjamin-Cummings (1985)